



## Original

# Interstitial pneumonia in immunocompetent laboratory rats caused by natural infection with *Pneumocystis carinii*

Masahiko YASUDA<sup>1</sup>, Ritsuki UCHIDA<sup>2,3</sup>, Yoko KAMAI<sup>1</sup>, Hanako MORITA<sup>2</sup>, Mai TANAKA<sup>2</sup>, Tomoko ISHIDA<sup>2</sup>, Misa MOCHIZUKI<sup>1</sup>, Masafumi YAMAMOTO<sup>2</sup>, Nobuhito HAYASHIMOTO<sup>2</sup> and Kenji KAWAI<sup>1</sup>

<sup>1</sup>Pathology Analysis Center, Central Institute for Experimental Animals, 3-25-12 Tonomachi, Kawasaki-ku, Kawasaki, Kanagawa 210-0821, Japan

<sup>2</sup>ICLAS Monitoring Center, Central Institute for Experimental Animals, 3-25-12 Tonomachi, Kawasaki-ku, Kawasaki, Kanagawa 210-0821, Japan

<sup>3</sup>JAC Inc., 1-2-7 Higashiyama, Meguro-ku, Tokyo 153-0043, Japan

**Abstract:** *Pneumocystis (P.) carinii* is known to cause fatal pneumonia in immunocompromised rats. Cases of *P. carinii* interstitial pneumonia in immunocompetent rats have been shown histologically to present with perivascular lymphoid cuffs, which have previously been attributed to rat respiratory virus. This study aims to determine the prevalence and pathological characteristics of *P. carinii* in immunocompetent laboratory rats in experimental facilities in Japan. An epidemiological survey for this agent was performed using PCR to assess 1,981 immunocompetent rats from 594 facilities in Japan. We observed that 6 of the 1,981 rats (0.30%) from 4 out of 594 facilities (0.67%) were positive for *P. carinii* without infection of other known pathogens. Gross pulmonary lesions were found in 4 of the 6 affected rats. The lungs of these rats contained scattered dark red/gray foci. Histopathologically, the lungs exhibited interstitial pneumonia with lymphoid perivascular cuffs: *Pneumocystis* cysts were observed using Grocott's methenamine silver stain. To our knowledge, this report is the first to reveal the prevalence of natural *P. carinii* infection in immunocompetent laboratory rats in Japan.

**Key words:** epidemiological survey, immunocompetent rats, *Pneumocystis carinii*

## Introduction

In the late 1990s, unexplained lymphohistiocytic interstitial pneumonia with perivascular lymphocytic cuffing was observed in immunocompetent rats used in toxicology studies. In 1997, the first report of lymphohistiocytic interstitial pneumonia was published under the title “Have you seen this?” [1], and two similar cases were successively reported [2, 3]. In the 2010s, several studies reported that opportunistic *Pneumocystis carinii* infection caused lymphohistiocytic interstitial pneumonia in immunocompetent rats [4–6]. *P. carinii* is well known as an opportunistic fungal pathogen that

causes lethal pneumonia in immunocompromised rats [7]. However, reports of *P. carinii* infection in immunocompetent rats are rare [8, 9], and the prevalence of *P. carinii* in rats worldwide and in Japan is unknown. Therefore, this study aims to investigate the prevalence of *P. carinii* in laboratory immunocompetent rats in experimental facilities in Japan and to characterize the pathophysiology of the infected lung tissues.

## Materials and Methods

A total 1,981 rats from 594 facilities (1,416 rats from 456 facilities in universities and research institutes, and

(Received 16 May 2021 / Accepted 11 August 2021 / Published online in J-STAGE 13 September 2021)

Corresponding author: M. Yasuda. email: myasuda@ciea.or.jp



This is an open-access article distributed under the terms of the Creative Commons Attribution Non-Commercial No Derivatives (by-nc-nd) License <<http://creativecommons.org/licenses/by-nc-nd/4.0/>>.

©2022 Japanese Association for Laboratory Animal Science

565 rats from 138 facilities in pharmaceutical companies and contract research organizations) within Japan were surveyed from November, 2013 to October, 2018. The rats were immunocompetent, and were sent to the ICLAS Monitoring Center for microbiologic monitoring, where they were euthanized with an overdose of isoflurane, investigated by necropsy, and assessed for infection with the following microorganisms: *Corynebacterium kutscheri*, *Mycoplasma (M.) pulmonis*, *Salmonella* spp., *Rodentibacter (R.) pneumotropicus*, *R. heyltii*, and *R. rattii* [*Pasteurella pneumotropica*] by culture; *Clostridium piliforme*, *M. pulmonis*, Sendai virus, Hantavirus, and Sialodacryoadenitis virus by serology; and intestinal protozoa, pinworms, and ectoparasites by microscopic observation. The protocol for this study was approved by the institutional animal care and use committee according to the Regulations for Animal Experimentation of CIEA.

From each rat, the right lung was used to test for *P. carinii* and the left lung was used for histopathological analysis. For detection of *P. carinii*, the right lung samples were homogenized, and DNA was extracted using a MagExtractor-Genome- (TOYOBO Co., LTD., Osaka, Japan) according to the manufacturer's instructions. *P. carinii* was identified genetically using the PCR primers pAZ112-10F (5'-TAG ACG GTC ACA GAG ATC AG -3') and pAZ112-10R (5'-GAA CGA TTA CTA GCA ATT CC-3'), which were designed based on the unique region of the mt SSU rRNA gene sequence of *P. carinii* [10]. The expected PCR product size is 706 bp. All PCR products in *P. carinii* PCR tests were directly sequenced and compared with the data available in a public database (GenBank) for verification.

Cultures from rats with gross lung lesions were prepared by directly streaking the cut surface of the right caudal lung lobe onto 5% horse blood agar (Eiken Chemical Co., Ltd., Tokyo, Japan) and PPLO agar (BD Biosciences, Bedford, MA, USA) supplemented with horse serum and yeast extract for *M. pulmonis*. Blood agar was assessed after incubation under aerobic conditions at 37°C for 48 h, and PPLO agar was assessed after incubation under microaerobic conditions at 37°C

for 7 days. *P. carinii*-positive rats were also tested serologically for the presence of the following known associated pathogens: *Filobacterium rodentium* (cilia-associated respiratory bacillus), mouse adenovirus, mouse encephalomyelitis virus, mouse min virus, pneumonia virus of mice, and reovirus type 3.

### Histopathological examination

For histopathological analysis, all left lobe of lungs was collected in 10% neutral-buffered formalin, embedded in paraffin, and sectioned into 4- $\mu$ m-thick slices. If gross lung lesions were observed, the nasal cavities and tracheas were also collected and sectioned as described above. These samples were stained using hematoxylin-eosin (HE), periodic acid-Schiff (PAS) reaction and Grocott-Gomori methenamine silver and Giemsa double (Grocott-Giemsa) staining [11] for examination by light microscopy. To characterize the lymphocytic infiltrates in lesions, immunohistochemical staining was performed using a Leica BOND-MAX automated IHC/ISH stainer and a Leica Polymer Refine detection kit (Leica Biosystems K.K., Tokyo, Japan) according to the manufacturer's instructions. Tissue sections were incubated with primary antibody diluted with Bond Primary Antibody Diluent (Leica Biosystems), as detailed in Table 1.

## Results

### Prevalence of *P. carinii*

PCR results showed that of the 1,416 rats from 456 facilities in universities and research institutes, 6 rats from 4 facilities were positive for *P. carinii* (Table 2). Of the 41 tested rats from 4 universities, the positivity for *P. carinii* was as follows: the university A, 1/14; university B, 1/14; university C, 3/6; and university D, 1/7. No *P. carinii* was found in any of the 565 rats from 138 facilities in pharmaceutical companies. Therefore, the overall prevalence of *P. carinii* was 0.30% (6/1,981) in immunocompetent laboratory rats and 0.67% (4/594) in rat facilities in Japan. PCR analysis of all 6 *P. carinii*-positive rats showed 99–100% similarity with the sequence data of the mt SSU rRNA gene of *P. carinii*. In

**Table 1.** Protocol used for each primary antibody

Lymphocyte	Antibody	Host	Clone	Dilution	Retrieval	Source <sup>c)</sup>
T-cell	CD3	Rabbit	SP7	1:50	ER1 <sup>a)</sup>	Nichirei
T-cell	CD4	Rabbit	D7D2Z	1:200	ER2 <sup>b)</sup>	Cell Signaling
T-cell	CD8 $\alpha$	Mouse	OX-8	1:200	ER1 <sup>a)</sup>	Abcam
B-cell	CD79 $\alpha$	Mouse	HM57	1:2	ER1 <sup>a)</sup>	Nichirei

<sup>a)</sup>Treated with ER1 (Citrate-based pH6.0 epitope retrieval solution; Leica Biosystems K.K., Tokyo, Japan) for 30 min at 100°C. <sup>b)</sup>Treated with ER2 (EDTA-based pH9.0 epitope retrieval solution; Leica Biosystems) for 20 min at 100°C.

<sup>c)</sup>Sources: Nichirei Biosciences, Inc. (Tokyo, Japan), Cell Signaling Technology, Inc. (Danvers, MA, USA), Abcam plc (Cambridge, UK).

addition, all 6 *P. carinii*-positive rats were negative for other pathogens.

**Gross and histopathological analysis of lesions**

At necropsy, four of the six *P. carinii*-positive rats had gross lung lesions. Two of the three *P. carinii*-positive rats from university C had no gross lesions (Table 3). The lungs of the four *P. carinii*-positive rats had dark red mottling with multiple dark red/gray foci (about 1 mm) in both lobes of the lung (Fig. 1). Furthermore, 10 of the *P. carinii*-negative rats from 10 facilities had other gross pulmonary lesions: 6 had well-circumscribed white/gray foci, histologically diagnosed as spontaneous alveolar macrophage accumulation; 2 had well-circumscribed dark red foci, histologically diagnosed as spontaneous congestion; one had congestion and red hepatization, diagnosed as murine respiratory mycoplasmosis associated with *M. pulmonis*; and one Brown Norway rat had multiple defined dark red foci histologically diagnosed as strain-specific eosinophilic granulomatous pneumonia. No clinical symptoms were noted in any of the rats, including those that were *P. carinii*-positive,

and no abnormalities were observed in any other organs.

Histopathologically, four of the six *P. carinii*-positive immunocompetent rats with pulmonary lesions were observed to have multifocal lymphohistiocytic perivascularitis and interstitial pneumonia (Table 4). Pulmonary lesions were primarily located in the lobules, not broncho- or bronchiolo-centric regions. No changes were found in the nasal cavity and trachea. Prominent dense perivascular infiltrates were observed throughout the lungs. Lymphocytes and macrophages significantly infiltrated to encircle the pulmonary and bronchial veins

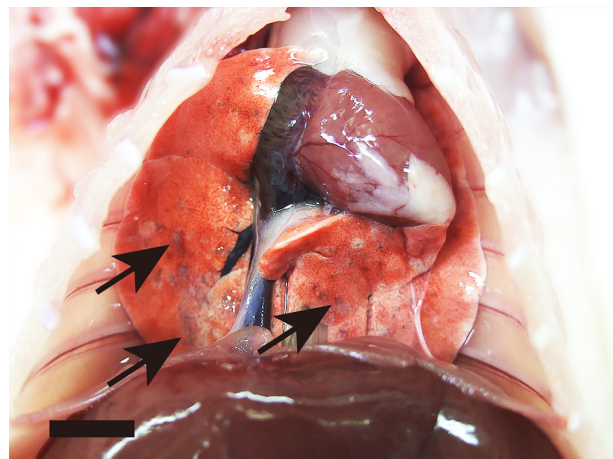


**Fig. 1.** Necropsy findings in the lung of a *P. carinii*-positive rat (from university C, #3). All lobes of the lung are slightly distended and have reddish discoloration and scattered dark red/grayish foci (arrows, bar: 10 mm).

**Table 2.** The positivity for *P. carinii* in rats according to facility

	Facilities	Rats
Academic	4/456 (0.88%)	6/1,416 (0.42%)
Commercial	0/138 (0%)	0/565 (0%)
Total	4/594 (0.67%)	6/1,981 (0.30%)

**Table 3.** Detailed information on *P. carinii*-positive rats

No.	Facilities	Strain	Sex	Age	<i>P. carinii</i> PCR test	Positivity for <i>P. carinii</i>
1	University A	Wistar	Male	11 weeks	Positive	1/14
2	University B	SD	Male	13 weeks	Positive	1/14
3	University C	Wistar	Female	Unknown	Positive	3/6
4		Wistar	Female	Unknown	Positive	
5		Wistar	Female	Unknown	Positive	
6	University D	Wistar	Female	22 weeks	Positive	1/7

**Table 4.** Pathological lesions in the lungs of *P. carinii*-positive rats

No.	Gross lesions	Microscopic lesions	Grocott-positive cysts
1	Multiple dark red foci	Multifocal lymphohistiocytic perivascularitis and mild granulomas	Detection of cysts attached to the alveolar epithelium
2	Multiple dark red foci	Multifocal lymphohistiocytic perivascularitis and mild granulomas	Detection of cysts attached to the alveolar epithelium
3	Multiple gray/dark red foci	Multifocal lymphohistiocytic perivascularitis and severe granulomas	Detection of cysts attached to the alveolar epithelium
4	No gross lesions	No abnormality	Non-detected
5	No gross lesions	No abnormality	Non-detected
6	Multiple dark red foci	Multifocal lymphohistiocytic perivascularitis and mild granulomas	Detection of cysts attached to the alveolar epithelium

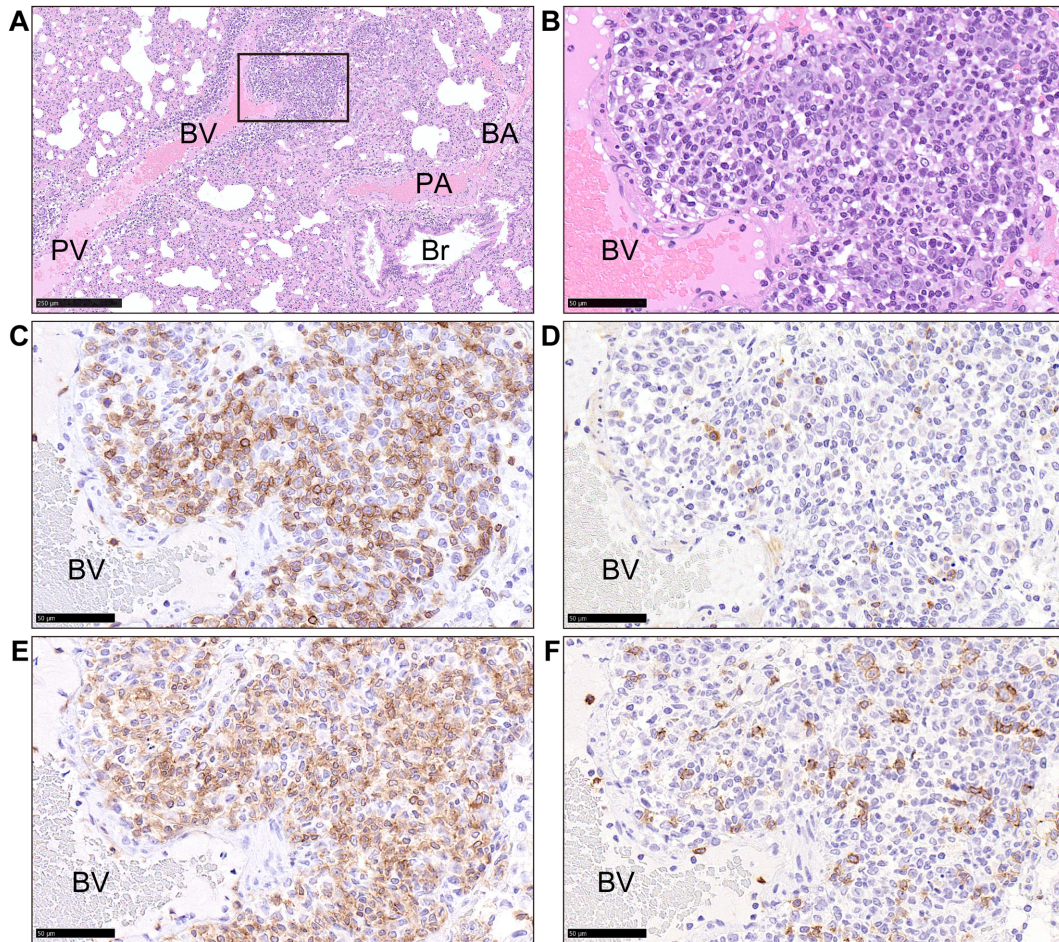


**Fig. 2.** Histopathological and immunohistochemical analysis of perivascular lesions in the lung of rat #3. Infiltrations of lymphocytes and macrophages are seen around the intrapulmonary vasculature, especially the bronchial vein (A and B). Most of the lymphocytes infiltrating the perivascular area are CD4-positive, CD8-negative T-cells (C–F). A) HE stain, bar: 250  $\mu\text{m}$ ; B) Magnified image of the square in A. HE stain, bar: 50  $\mu\text{m}$ ; C) CD3 immunostain, bar: 50  $\mu\text{m}$ ; D) CD79 $\alpha$  immunostain, bar: 50  $\mu\text{m}$ ; E) CD4 immunostain, bar: 50  $\mu\text{m}$ ; F) CD8 $\alpha$  immunostain, bar: 50  $\mu\text{m}$ ; BA, bronchial artery; Br, bronchus; BV, bronchial vein; PA, pulmonary artery; PV, pulmonary vein.

(Figs. 2A and B). Significant hyperplasia of bronchus-associated lymphoid tissue (BALT) was not observed. Most of these infiltrated lymphocytes were CD3-positive T-cells, of which most were CD4-positive and CD8-negative, and CD79 $\alpha$ -positive B-cell infiltration was low (Figs. 2C–F). Thickened alveolar septa infiltrated lymphocytes and macrophages, loss of type I pneumocytes, and proliferation of enlarged type II pneumocytes were observed in the alveolar areas. Most of the lymphocytes infiltrating the alveolar walls were CD3-positive T-cells. Some alveolar lesions were mild-to-severe granulomas (Figs. 3A and B), and large foamy macrophages infiltrated the alveolar spaces, but the cytoplasm of macrophages was PAS negative. Furthermore, a few fungus-like structures disclosed by Grocott–Giemsa staining were observed in the alveoli distant from the lymphocytic cuffs (Fig. 4A). These 3–5  $\mu\text{m}$ -diameter structures were round-, bowl-, or crescent-shaped with a black-

stained wall. Some of the fungus-like structures had an intracystic dot. Based on these characteristic findings, the structures were determined to be cysts of *Pneumocystis*. In the region of the lobe, thickening of the alveolar septa was observed, but inflammatory cell infiltration was mild (Fig. 4B). These cysts were found attached to type I pneumocytes or in the interstitial tissues (Figs. 4C and D). However, Grocott staining-positive cysts were found only upon careful inspection, with only a few observed in each lung tissue section.

Based on the above findings, the diagnosis of these lung lesions in immunocompetent rats was interstitial pneumonia caused by *P. carinii* infection. The gross and histopathological findings of the pulmonary lesions were nearly identical between the 4 *P. carinii*-positive rats.

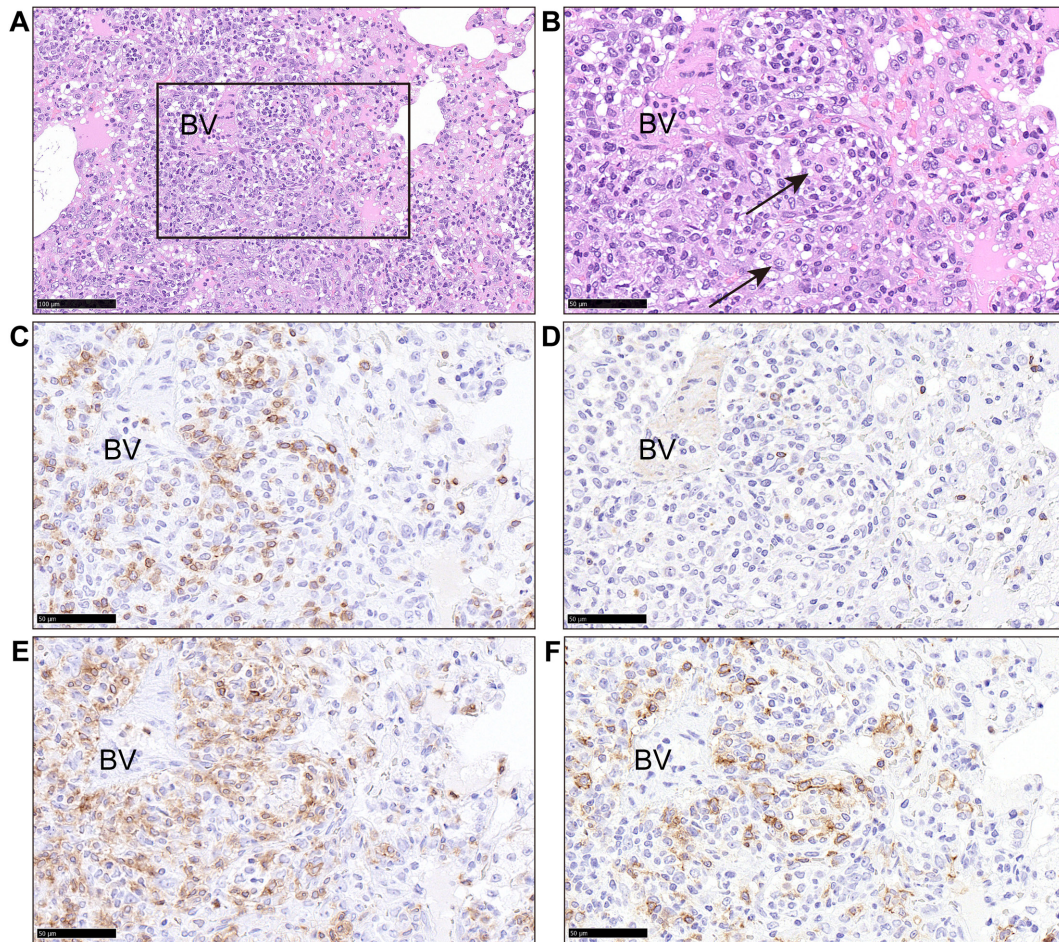


**Fig. 3.** Histopathological and immunohistochemical analysis of lobular lesions in the lung of rat #3. In the lobular region near the BV (A and B) at the site of CD3-positive T-cell infiltration (B and C), the alveolar structures are collapsed, with loss of type I pneumocysts; granulomas are present (B; arrows). In the pulmonary interstitium, infiltrations of lymphocytes are comparable in CD4- and CD8-positive T-cells (E and F). A) HE stain, bar: 250  $\mu$ m; B) Magnified image of the square in A. HE stain, bar: 50  $\mu$ m; C) CD3 immunostain, bar: 50  $\mu$ m; D) CD79 $\alpha$  immunostain, bar: 50  $\mu$ m; E) CD4 immunostain, bar: 50  $\mu$ m; F) CD8 $\alpha$  immunostain, bar: 50  $\mu$ m.

## Discussion

*Pneumocystis* species are not often among the common infectious agents recommended for screening of immunocompetent rats housed in laboratories but are included among additional agents for monitoring. Widespread *P. carinii* infection in the North American commercial immunocompetent rat colonies was reported in the 1990s [12–14], but the prevalence of *P. carinii* in Japan was previously unknown. This study showed for the first time that the overall prevalence of *P. carinii* was 0.30% in immunocompetent laboratory rats and 0.67% in rat facilities in Japan. Until 2011, lung lesions in immunocompetent rats infected with *P. carinii* had been attributed to rat respiratory virus (RRV) [4, 6, 15, 16]. In 2002, the positivity rate of “RRV” findings in immunocompetent rats was 6.36% as determined by histopathological tests of the lungs [9]; in immunodeficient

rats, the rate was about 4.0% [8]. Therefore, these findings suggest that in the early 2000s, the positivity rate of *P. carinii* was high in North America. In contrast, the positivity rate of *P. carinii* in Japan at that time was 0% (not detected by health monitoring tests of sentinel immunocompetent rats) in laboratory immunodeficient rat colonies [17].

The histopathological characteristics of apparent *P. carinii* pneumonia in immunocompetent rats are the same as those described by Albers, *et al.* [18] to diagnose RRV infectious interstitial pneumonia, as follows: (1) dense cuffs of lymphocytes admixed with lesser numbers of macrophages and plasma cells around multiple vessels in multiple areas of the lung; (2) thickening of the adjacent alveolar septa by lymphohistiocytic infiltration; and (3) nonspecific lesions including hyperplasia of BALT and infiltration into/around the bronchus. The pulmonary lesions in four of the cases reported here met these his-

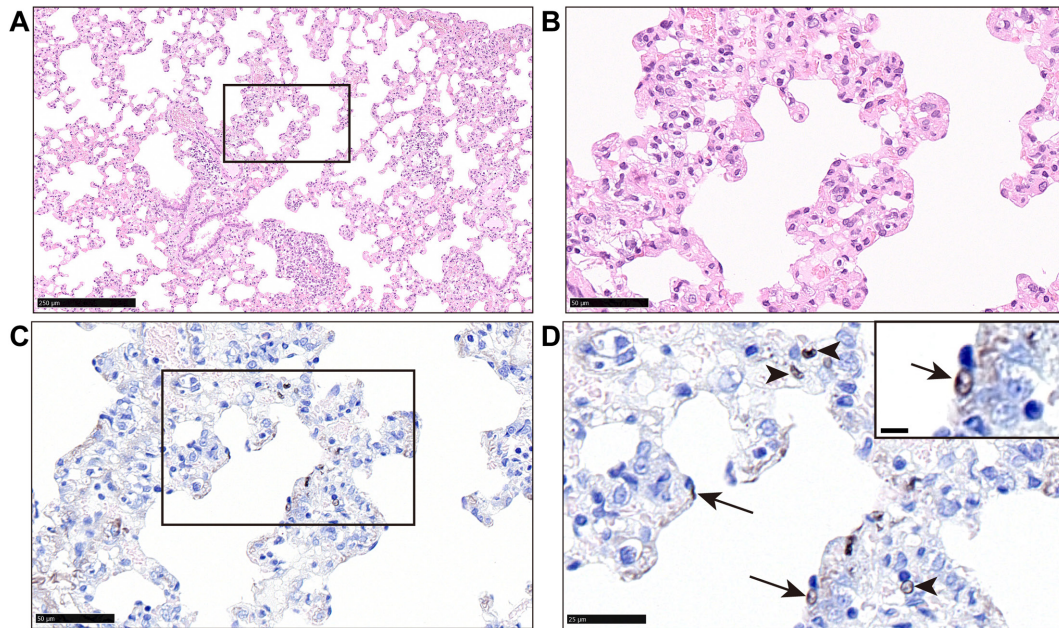


**Fig. 4.** Histopathological analysis of the alveolar region in the lung of rat #3. In alveoli with enlarged pneumocysts and macrophage infiltration, Grocott-positive fungal-like structures are observed adhering to the alveolar walls (arrows) and the alveolar interstitium (arrowheads). The longest cyst diameter is about 5  $\mu\text{m}$  (D; inset). A) HE stain, bar: 250  $\mu\text{m}$ ; B) Magnified image of the square in A. HE stain, bar: 50  $\mu\text{m}$ ; C) Grocott–Giemsa stain, bar: 50  $\mu\text{m}$ ; D) Magnified image of the square in C. Grocott–Giemsa stain, bar: 25  $\mu\text{m}$  (bar in inset: 5  $\mu\text{m}$ ).

topathological criteria. In addition, these cases showed Grocott–Giemsa staining of cyst walls and were PCR positive for *P. carinii*. Thus, these pulmonary lesions were histopathologically diagnosed as lymphohistiocytic interstitial pneumonia in immunocompetent rats resulting from *P. carinii* infection. In these cases, the lesions were characteristic of lymphocytic infiltration around pulmonary vessels without hyperplasia of BALT. This perivascular lymphocytic infiltrate mainly consisted of CD4-positive T-cells. Similar lesions have been reported in human pneumocystis pneumonia [19]. This finding suggests that *P. carinii*-infected immunocompetent rats may be a good non-immunocompromised model of *P. jirovecii* infection in humans. This study is the first to report the incidence and pathological features of a natural *P. carinii* infection in immunocompetent laboratory rats in Japan. While the prevalence of *P. carinii* in Japan is very low, reports indicate that immunocompetent hosts may play an important role in the *Pneumocystis* life cycle in humans [20, 21], laboratory mice [20] and rats [4, 6, 22], and that immunocompetent laboratory rats may be carriers of *Pneumocystis* infection. Consequently, *Pneumocystis* should be considered as a microbe that can cause opportunistic infection in immunocompetent laboratory animals.

## Acknowledgments

The authors declare no conflicts of interests associated with this manuscript and would like to thank the staff at the ICLAS monitoring center at CIEA for research assistance. Finally, the authors are also grateful to Enago for proofreading this manuscript.

## References

1. Elwell MR, Mahler JF, Rao GN. "Have you seen this?" Inflammatory lesions in the lungs of rats. *Toxicol Pathol.* 1997; 25: 529–531. [Medline] [CrossRef]
2. Gilbert BE, Black MB, Waldrep JC, Bennick J, Montgomery C, Knight V. Cyclosporin A liposome aerosol: lack of acute toxicity in rats with a high incidence of underlying pneumonitis. *Inhal Toxicol.* 1997; 9: 717–730. [CrossRef]
3. Slaoui M, Dreef HC, van Esch E. Inflammatory lesions in the lungs of Wistar rats. *Toxicol Pathol.* 1998; 26: 712–713, discussion 714. [Medline] [CrossRef]
4. Henderson KS, Dole V, Parker NJ, Momtsios P, Banu L, Brouillette R, et al. *Pneumocystis carinii* causes a distinctive interstitial pneumonia in immunocompetent laboratory rats that had been attributed to "rat respiratory virus". *Vet Pathol.* 2012; 49: 440–452. [Medline] [CrossRef]
5. Kim HS, Do SI, Kim YW. Histopathology of *Pneumocystis carinii* pneumonia in immunocompetent laboratory rats. *Exp Ther Med.* 2014; 8: 442–446. [Medline] [CrossRef]
6. Livingston RS, Besch-Williford CL, Myles MH, Franklin CL, Crim MJ, Riley LK. *Pneumocystis carinii* infection causes lung lesions historically attributed to rat respiratory virus.

- Comp Med. 2011; 61: 45–59. [\[Medline\]](#)
7. Frenkel JK, Good JT, Shultz JA. Latent *Pneumocystis* infection of rats, relapse, and chemotherapy. *Lab Invest.* 1966; 15: 1559–1577. [\[Medline\]](#)
  8. Livingston RS, Riley LK. Diagnostic testing of mouse and rat colonies for infectious agents. *Lab Anim (NY).* 2003; 32: 44–51. [\[Medline\]](#) [\[CrossRef\]](#)
  9. Pritchett-Corning KR, Cosentino J, Clifford CB. Contemporary prevalence of infectious agents in laboratory mice and rats. *Lab Anim.* 2009; 43: 165–173. [\[Medline\]](#) [\[CrossRef\]](#)
  10. Hunter JAC, Wakefield AE. Genetic divergence at the mitochondrial small subunit ribosomal RNA gene among isolates of *Pneumocystis carinii* from five mammalian host species. *J Eukaryot Microbiol.* 1996; 43: 24S–25S. [\[Medline\]](#) [\[CrossRef\]](#)
  11. Shiota T. Simultaneous demonstration of cyst walls and intracystic bodies of *Pneumocystis carinii* in paraffin embedded lung sections using Gomori's methenamine silver nitrate and Giemsa stain. *J Clin Pathol.* 1986; 39: 1269–1271. [\[Medline\]](#) [\[CrossRef\]](#)
  12. Cushion MT, Kaselis M, Stringer SL, Stringer JR. Genetic stability and diversity of *Pneumocystis carinii* infecting rat colonies. *Infect Immun.* 1993; 61: 4801–4813. [\[Medline\]](#) [\[CrossRef\]](#)
  13. Icenhour CR, Rebholz SL, Collins MS, Cushion MT. Widespread occurrence of *Pneumocystis carinii* in commercial rat colonies detected using targeted PCR and oral swabs. *J Clin Microbiol.* 2001; 39: 3437–3441. [\[Medline\]](#) [\[CrossRef\]](#)
  14. Weisbroth SH, Geistfeld J, Weisbroth SP, Williams B, Feldman SH, Linke MJ, et al. Latent *Pneumocystis carinii* infection in commercial rat colonies: comparison of inductive immunosuppressants plus histopathology, PCR, and serology as detection methods. *J Clin Microbiol.* 1999; 37: 1441–1446. [\[Medline\]](#) [\[CrossRef\]](#)
  15. Riley LK, Purdy G, Dodds J, Franklin CL, Besch-Williford C, Hook RR Jr, et al. Idiopathic lung lesions in rats: search for an etiologic agent. *Contemp Top Lab Anim Sci.* 1997; 36: 46. [\[Medline\]](#) [\[CrossRef\]](#)
  16. Riley LK, Simmons JH, Purdy G, Livingston R, Franklin C, Besch-Williford C. Research update: idiopathic lung lesions in rats. *ACLAD News.* 1999; 20: 9–11.
  17. Hayashimoto N, Morita H, Ishida T, Yasuda M, Kameda S, Uchida R, et al. Current microbiological status of laboratory mice and rats in experimental facilities in Japan. *Exp Anim.* 2013; 62: 41–48. [\[Medline\]](#) [\[CrossRef\]](#)
  18. Albers TM, Simon MA, Clifford CB. Histopathology of naturally transmitted “rat respiratory virus”: progression of lesions and proposed diagnostic criteria. *Vet Pathol.* 2009; 46: 992–999. [\[Medline\]](#) [\[CrossRef\]](#)
  19. Hoving JC, Kolls JK. New advances in understanding the host immune response to *Pneumocystis*. *Curr Opin Microbiol.* 2017; 40: 65–71. [\[Medline\]](#) [\[CrossRef\]](#)
  20. Dumoulin A, Mazars E, Seguy N, Gargallo-Viola D, Vargas S, Cailliez JC, et al. Transmission of *Pneumocystis carinii* disease from immunocompetent contacts of infected hosts to susceptible hosts. *Eur J Clin Microbiol Infect Dis.* 2000; 19: 671–678. [\[Medline\]](#) [\[CrossRef\]](#)
  21. Vargas SL, Ponce CA, Gigliotti F, Ulloa AV, Prieto S, Muñoz MP, et al. Transmission of *Pneumocystis carinii* DNA from a patient with *P. carinii* pneumonia to immunocompetent contact health care workers. *J Clin Microbiol.* 2000; 38: 1536–1538. [\[Medline\]](#) [\[CrossRef\]](#)
  22. Menotti J, Emmanuel A, Bouchekouk C, Chabe M, Choukri F, Pottier M, et al. Evidence of airborne excretion of *Pneumocystis carinii* during infection in immunocompetent rats. Lung involvement and antibody response. *PLoS One.* 2013; 8: e62155. [\[Medline\]](#) [\[CrossRef\]](#)